NRC Publications Archive
Archives des publications du CNRC

Modeling the Thermal Effect of the Bipolar Electrocautery for Neurosurgery Simulation

Delorme, Sébastien; Cabral, Anne; Ayres, Fabio; Jiang, Di

NRC Publications Record / Notice d'Archives des publications de CNRC:
https://nrc-publications.canada.ca/eng/view/object/?id=b9307d2e-199e-444e-8c3f-fab11271d490
https://publications-cnrc.canada.ca/fra/voir/objet/?id=b9307d2e-199e-444e-8c3f-fab11271d490

Questions? Contact the NRC Publications Archive team at
PublicationsArchive-ArchivesPublications@nrc-cnrc.gc.ca. If you wish to email the authors directly, please see the first page of the publication for their contact information.

Vous avez des questions? Nous pouvons vous aider. Pour communiquer directement avec un auteur, consultez la première page de la revue dans laquelle son article a été publié afin de trouver ses coordonnées. Si vous n'arrivez pas à les repérer, communiquez avec nous à PublicationsArchive-ArchivesPublications@nrc-cnrc.gc.ca.

National Research Council Canada   Conseil national de recherches Canada

Canada

Modeling the Thermal Effect of the Bipolar Electrocautery for Neurosurgery Simulation

Sébastien DELORME [1], Anne CABRAL, Fábio AYRES, and Di JIANG
Industrial Materials Institute, National Research Council Canada

Abstract. Real-time surgical simulation requires computationally-fast models describing the interaction between surgical instrument and tissues. In this study, a model for predicting the temperature distribution in brain tissue when using a bipolar electrocautery is proposed and validated against experimental *in vitro* animal data. Joule heat generation and heat conduction in the tissue are considered. The agreement between simulated temperature distributions and experimental data could be improved by modeling the output power as a function of electrical resistance between the electrodes, and by considering the heat exchange with surrounding air and bipolar tips.

Keywords. Neurosurgery, simulation, electrocautery.

Introduction

Surgical simulation requires modeling the interaction between surgical tools and biological tissues. In neurosurgery, the bipolar electrocautery (Figure 1) has become an essential tool for control of bleeding by coagulating tissues and blood vessels [1]. Its two metallic tips are electrodes connected to a high-frequency sine wave generator. When alternating current is applied and both tips are in contact with tissue, the area around the tips heats up. Temperatures up to 80°C have been measured on liver tissue after 10 seconds of electric current application [2]. Coagulation is achieved in areas that have exceeded a critical temperature. After cauterization, small but visible blood vessels disappear, while vascularised tissues become less pink. Unintended heat transfer into the surrounding tissues can result in unwanted thermal damage to blood vessels or brain tissue. Simulators can help learning how to safely use the bipolar cautery near critical areas, a common scenario in neurosurgery.

Figure 1. Bipolar electrocautery handle.

The objective of this study is to model the shape and extent of the cauterized area, as a function of controllable factors such as applied electrical power, duration of electrical power application, and distance between the electrode tips. A validation of the simulation results against *in vitro* experimental data is presented. Implementations of the model for real-time computation in a surgical simulator are discussed.

1. Methodology

1.1. Numerical Model

Two phenomena involved in the cauterization with a bipolar were considered in the numerical simulations: Joule heating and heat conduction in the tissue. When an electrical field is created inside brain tissue, heat is generated according to

$$\dot{Q} = \frac{\|\vec{J}\|^2}{\sigma} \tag{1}$$

where $\dot{Q}$ is the time rate of heat generated per unit of volume [W/m^3], σ is electrical conductivity, and $\vec{J}$ is electrical current density [A/m^2]. Assuming perfect contact between the electrodes and the tissue, the current density at any point P can be obtained by superposition of current density for each electrode

$$\vec{J} = \frac{I}{2\pi\|\vec{r_+}\|^2} \times \frac{\vec{r_+}}{\|\vec{r_+}\|} - \frac{I}{2\pi\|\vec{r_-}\|^2} \times \frac{\vec{r_-}}{\|\vec{r_-}\|} \tag{2}$$

where I is the electrical current intensity, $\vec{r_+}$ is the vector from the positive electrode to point P, and $\vec{r_-}$ is the vector from the negative electrode to point P (Figure 2). The temperature distribution in space and time $T(x, y, z, t)$ can be computed by solving the heat conduction equation

$$\rho c \frac{\partial T}{\partial t} = \nabla \cdot (k \nabla T) + \dot{Q} \tag{3}$$

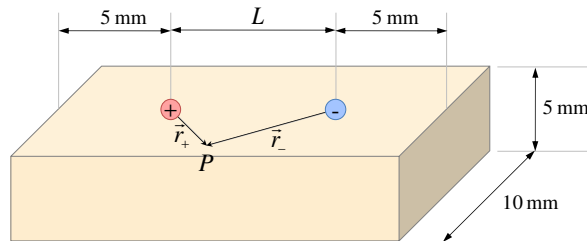where ρ is mass density, c is specific heat capacity, and k is thermal conductivity.

Figure 2. Computation domain dimensions, electrodes position, and vectors definition for Eq. (2).

Temperature was integrated over time using a finite difference explicit scheme, over a 3D domain of 5 by 10 by $(10 + L)$ mm, where L is the distance between the electrodes centers (Figure 2), divided in a regular grid with 0.2 mm steps between nodes (approximately 100,000 nodes depending on L). The second derivative was approximated by a second order central difference (MatLab `del2` function), which uses cubic extrapolation of the temperature for the boundary nodes of the domain.

Electrocautery generators allow setting a nominal power and will control the duration of alternate current bursts at constant voltage to obtain the desired average output power at a nominal resistance value. If the resistance between the electrodes is different than the nominal resistance, the output power will be less than the nominal power [4]. Such behavior is expected: one could model a real voltage source as an ideal constant voltage source with an internal resistance to account for power losses in the voltage generating equipment. In that case, the maximum output power is given when the load resistance matches the internal resistance.

The electrical current intensity was calculated from the nominal power P using

$$I = \sqrt{\frac{P}{R}} \tag{4}$$

where R is an estimate of the equivalent electrical resistance of the tissue obtained by

$$R = \frac{V}{I} = \frac{1}{I} \int_{r_e}^{L} \frac{\|\vec{J}\|}{\sigma} dx = \frac{1}{2\pi\sigma} \left(\frac{1}{r_e} - \frac{1}{L - r_e} \right) \tag{5}$$

where r_e is the radius of the electrode tips. The electrodes tips were centered on the tissue-air boundary of the computation domain. The electrode tips were assumed to be hemispherical and penetrating the tissue by a distance r_e. Therefore a zero electrical current density was imposed at all nodes within a distance r_e from the electrode center. Heat transfer outside of the tissues (e.g. electrodes, air) was not considered.

To ensure convergence of the finite difference time-domain integration, time steps were defined using the following Courant-Friedrichs-Lewy condition in 3D [3]:

$$\Delta t \leq \frac{\rho c}{6k} \Delta x^2 \tag{6}$$

The following physical constants were used: $\sigma = 0.19\ \Omega^{-1}{\cdot}m^{-1}$ *in vitro* at $T{=}37°C$, with 1.75% increase per °C ; $\rho = 1.04{\times}10^3$ kg/m^3 ; $c = 3.6{\times}10^3$ J/kg·K ; and $k = 0.5$ W/m·K.

In a simulation of an *in vivo* situation, the physiological tissue temperature ($T_0 = 37°C$) would be applied as the initial condition over the entire domain and as the boundary condition on all boundaries of the domain except the brain-air interface. For *in vitro*, a different temperature could be used to match the experimental conditions. To simulate vaporization of the water content of tissues, temperatures were limited to 100°C, and at nodes that have reached such temperature Joule heating was fully cancelled by latent heat absorption.

1.2. In Vitro Experiments

In vitro experiments were done to measure the thermal effect of the bipolar electrocautery on animal brain. An infrared camera (SC620, FLIR Systems Inc), a digital video camera (HDR-XR200 AVCHD Handycam, Sony) and a bipolar electrocautery handpiece (22.5 cm Stainless Steel Bipolar Bayonet Forceps, Medicon), connected to an electrosurgical generator (GN060 Bipolar Coagulator, Aesculap), were mounted over a specimen platform (Figure 3). The specimen platform had macro and micro height adjustment. The bipolar handpiece was tilted 30 degrees from vertical to allow thermal imaging vertically.

Three fresh brains from 3-month old calves obtained from a slaughterhouse were tested within 4 hours post-mortem. Upon arrival at the laboratory, the brains were maintained at body temperature in a heated bath of phosphate buffered saline solution. A brain was then placed in a plastic dish on the specimen platform. The platform was raised until the two tips of the bipolar were in contact with the brain surface. The distance between the bipolar tips was set to a desired value using an adjustable spacer. The power on the generator was set to a desired nominal value. While recording with the two cameras, the power was activated using a foot pedal for 10 seconds. After the recording was stopped, the specimen platform was lowered, and the dish was moved in order to perform another test at a different location at least 20 mm away from any other testing area. When no more areas were available for testing, another brain was taken out of the heated bath for testing. Throughout the experiment, the brain was kept wet and the bipolar was kept clean of adhered tissue. Testing conditions selected to highlight the effect of nominal power, distance between bipolar tips, and duration, are described in Table 1.
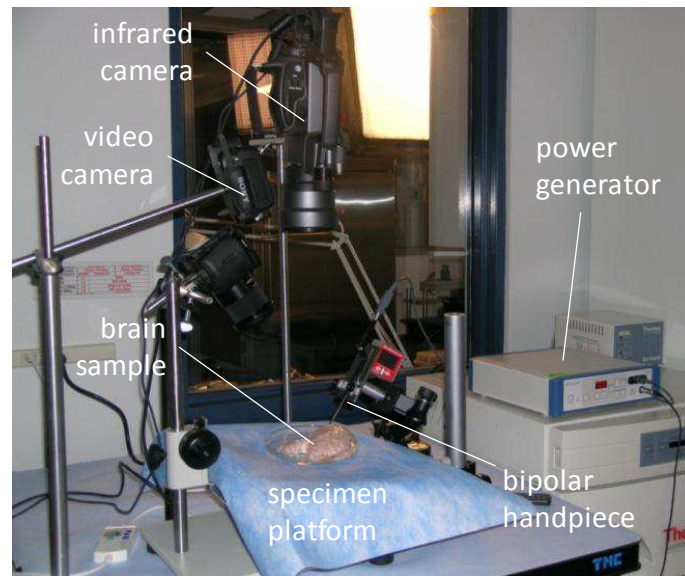

Figure 3. Experimental setup

Table 1. Testing conditions

Parameter	Symbol	Test 1	Test 2	Test 3	Test 4
Electrode tip radius	r_e	0.5 mm	0.5 mm	0.5 mm	0.5 mm
Duration of power application	T	3 sec	3 sec	10 sec	3 sec
Nominal power on generator	P	13 W	5 W	5 W	13 W
Distance between electrode tips	L	3 mm	3 mm	3 mm	6 mm

2. Results

Simulations were run under the same conditions as the selected *in vitro* experiments. The initial tissue temperature was set in the simulations to the average measured tissue temperature before applying electrical power. Simulated and experimental temperature distributions on the tissue-air boundary plane are showed in Figure 4.

3. Discussion

3.1. Experimental Validation of the Simulation

Simulation with nominal power resulted in hotter temperature profiles than experimentally measured. Bipolar generators are designed to output variable power depending on electrical resistance between the electrodes. The output power matches the set power when resistance is approximately between 50 and 100 Ω, for the generator used in this experiment [4]. In our experiment, the electrical resistance was not measured. In the simulations we used brain resistivity data from the literature, which varies between sources as well as between *in vivo* and *in vitro* conditions [5][6]. Resistance is also affected by the contact area between the electrode and the tissue. In our simulations, we assumed perfect contact over the surface of the electrode tip, whereas in the experiments the electrodes were at an angle and contact force was difficult to control due to viscoelasticity of brain tissue. Although tissues were kept moist by periodical irrigation with PBS, tissue moisture, which also has an impact on electrical resistance, might have varied during and between experiments. Furthermore, the presence of pia mater over the grey matter might also have altered the effective electrical resistance between electrodes.

Therefore, the power was adjusted until the simulated temperature at the midpoint between the electrodes matched that of the experiment, in order to simulate a situation where the electrical resistance between the electrodes would have been measured. The simulated temperature distribution profile with the adjusted power better matched the experimental results. However, the tissue was too hot near the electrodes and fell too fast away from the probe.
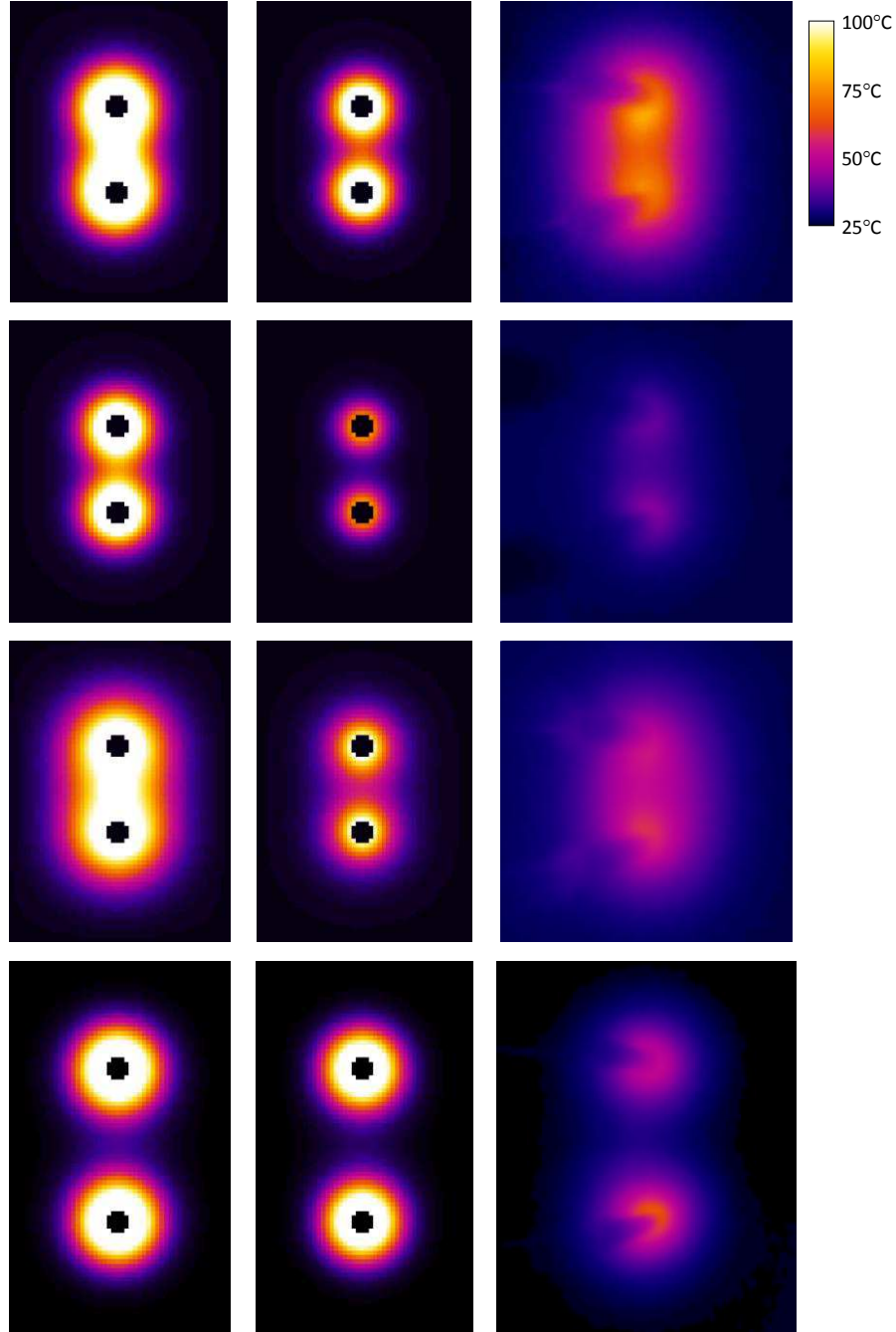
Figure 4. Simulated temperature distribution on the tissue-air plane at nominal power (column 1), at adjusted power (column 2), and experimental results (column 3), for the following testing conditions: $P_{nominal}$ = 13 W, L = 3 mm, and t = 3 sec (line 1); $P_{nominal}$ = 5 W, L = 3 mm, and t = 3 sec (line 2); $P_{nominal}$ = 5 W, L = 3 mm, and t = 10 sec (line 3); $P_{nominal}$ = 13 W, L = 6 mm, and t = 3 sec (line 4). All results are displayed with the same color map (top right).

Experiments with measurement of output power or of electrical resistance between the electrodes must be done to further validate these results and identify potential model improvements.

In the simulations, the limit temperature of 100℃ was reached in nodes close to the electrodes. However, the experimental results rarely showed maximum temperatures of 100℃. Apart from measurement errors, this could be due to other potential thermal phenomena that were not considered in the simulation, such as heat conduction from the tissue to the electrodes, as well as heat conduction and convection from the tissue to the air. Simulation of some of these phenomenon increases considerably the computational burden because it requires drastically smaller time steps to satisfy the CFL condition of Eq. (6). Nevertheless, each of these phenomena is expected to generate tissue temperatures cooler than in our simulations. Although the brain specimen were not perfused during the *in vitro* experiments, heat dissipation due to blood perfusion is expected to further cool tissues *in vivo*, and might have an important enough effect to require modeling for simulating *in vivo* interaction of the bipolar electrocautery with brain tissue.

The effective electrode contact radius also has a significant impact on the current density which decreases approximately with the square of the distance from the electrode center. A locally denser mesh around the electrodes might have helped provide more accurate temperature distribution in this area, but local refinement is not possible with regular grid methods such as the finite difference method.

3.2. Implementation in Surgical Simulator

In a surgical simulator, the bipolar electrocautery can be moved around freely over the tissue surface during power application. The Joule heating phenomenon can be implemented for real time computation using a 3D core of a linear or non-linear heat injection profile over a voxelised domain, and superposition over time to account for the accumulation of thermal energy in the brain tissue. However, heat conduction continues after the bipolar has moved away from the heated area, which requires computing heat conduction over the whole simulated domain. Using the explicit scheme resolution of the heat conduction problem, the computational time was 15 times greater than the simulation time, over a domain limited to 5 mm distance around the bipolar tips. Future work will focus on proposing solutions for implementing real time computation of heat conduction.

References

[1] L.I. Malis, Electrosurgery, *J Neurosurg* **85** (1996), 970-975.
[2] E.W. Elliott-Lewis, A.M. Mason, D.L. Barrow, Evaluation of a new bipolar coagulation forceps in a thermal damage assessment, *Neurosurg* **65** (2009), 1182-1187.
[3] W.H. Press, S.A. Teukolsky, W.T. Vetterling, B.P. Flannery, *Numerical Recipes: The Art of Scientific Computing*, Cambridge University Press, New York, 2007.
[4] *High-frequency surgery unit GN 060, Instructions for use/Technical description*. http://www.aesculapusa.com/default.aspx?pageid=498, retrieved Nov 1, 2010.
[5] K.R. Foster, H.P. Schwan, Dielectric properties of tissues and biological materials: a critical review, *Crit Rev Biomed Eng* **17** (1989), 25–103.
[6] J. Latikka, T. Kuurne, H. Eskola, Conductivity of living intracranial tissues, *Phys Med Biol* **46** (2001), 1611–1616.